Kinetic Modeling of Exciton Migration in Photosynthetic Systems. 2. Simulations of Excitation Dynamics in Two-dimensional Photosystem I Core Antenna/Reaction Center Complexes[1,2]

Gediminas Trinkunas and Alfred R. Holzwarth
Max-Planck-Institut für Strahlenchemie, D-4330 Mülheim a.d. Ruhr, Germany

ABSTRACT Kinetic modeling of the exciton migration in the cyanobacterial photosystem I core complex from *Synechococcus* sp. was performed by an exact solution of the Pauli master equation for exciton motion. A square two-dimensional 10 × 10 pigment lattice and a Förster dipole-dipole coupling between chromophores was assumed. We calculated decay-associated spectra and lifetimes and compared them to the corresponding experimental data from picosecond fluorescence and transient absorption obtained by global analysis. Seven spectral chlorophyll (Chl) forms, identical in shape but shifted in their absorption maximums, were used to describe the non-homogeneous broadening of the PS I-100 particle absorption spectrum. The optimized Chl lattice arrangement best reproducing the experimental decay-associated spectra as well as the steady-state fluorescence spectrum indicated the long-wavelength-absorbing Chls forming a cluster in the corner of the lattice with the reaction center (RC) placed apart at a distance of two lattice constants. The variable parameters, i.e., the charge separation rate in the RC and the lattice constant **a**, were found to be optimal at k_{RC} = 2.3 ps^{-1} and **a** = 1.14 nm, respectively. The surprising conclusions of the simulations is that Chls with absorption maxima as long a 724 nm have to be taken into account to describe the time-resolved spectra of this PS I particle properly. The dependencies of the exciton decay in the model PS I particle on the excitation wavelength and on the temperature are discussed. We also show that the excited state decay of similar PS I particles that lack the long-wavelength absorbing Chls is nearly mono-exponential. Various critical factors that limit the general reliability of the conclusions of such simulations are discussed in detail.

INTRODUCTION

In photosynthetic organisms light energy is captured by antenna pigments. For organisms performing oxygenic photosynthesis, the major antenna pigments in the near vicinity of the reaction centers (RCs) are chlorophyll (Chl) a or Chl b molecules bound to proteins. The antenna complexes can be functionally and biochemically grouped into the core complexes, which form the immediate surrounding of the RCs, and the peripheral complexes, which are more distantly located from the RCs (van Grondelle and Amesz, 1986). A high-resolution x-ray structure has not been determined for any of the Chl core or peripheral antenna complexes of higher plants or other oxygenic photosynthetic organisms. The only high-resolution structure of a Chl antenna system reported is the so-called Fenna-Mathews-Olson bacterio-Chl, a protein complex isolated from the baseplates of chlorosomes from the green bacterium *Prosthecochloris aestuarii* (Matthews and Fenna, 1980). Two-dimensional electron micrography of the higher plant light-harvesting Chl a/b complex (LHC 2) has resulted in a structure resolution of about 3.5 Å (Kühlbrandt and Wang, 1991; Kühlbrandt and Downing, 1989). This resolution is not sufficient, however, to locate and identify all Chls or to precisely define their relative orientation. More recently, crystals have been obtained for the photosystem (PS) I core complex of the thermophilic cyanobacterium *Synechococcus* sp. (Rögner et al., 1990; Boekema et al., 1989; Witt et al., 1988; Krauss et al., 1993). The PS I core complex is composed of, inter alia, the RC structure of PS I, the primary and secondary electron acceptors and, intimately coupled to the RC, about 100 protein-bound Chl a molecules that form the antenna. The reported x-ray data for this complex have a resolution of about 6 Å (Krauss et al., 1993). Despite showing some interesting detail, this structural resolution is not yet sufficient to propose any detailed models as far as energy transfer is concerned.

The theoretical description of energy transfer processes in photosynthetic antennae is difficult. The first problem is the either nonexistent or, at best, incomplete information on structure. However, even having detailed structural information would not improve the situation. A key difficulty is the unsolved problem of chromophore/protein interactions which modify the spectral features of the Chl chromophores in an unknown manner and lead to non-homogeneous broadening effects (Lee et al., 1985; Friedrich and Haarer, 1984). There may be several different reasons for the non-homogeneous broadening in Chls, but the main reasons probably lie in the flexibility of the chlorin ring systems and in

Received for publication 4 June 1993 and in final form 10 November 1993.

Address reprint requests to Dr. Alfred R. Holzwarth, Max-Planck Institut für Strahlenchemie, Stiftstrasse 34–36, D-45470 Mülheim/Ruhr 1, Germany.

Dr. Trinkunas is on leave of absence from the Institute of Physics, Vilnius 2600, Lithuania.

Abbreviations used: Chl, chlorophyll; DAS, decay-associated spectrum; LWA pigment, long wavelength-absorbing pigment; RC, reaction center; P700, primary donor of PS I reaction center; RA, red aggregate.

[1] Part 1 of this paper was published as "Effects of pigment heterogeneity and antenna topography on exciton kinetics and charge separation yields" (Beauregard et al., 1991).

[2] Dedicated to Prof. W. Rüdiger on the occasion of his 60th birthday.

© 1994 by the Biophysical Society

0006-3495/94/02/415/15 $2.00

the differential protein interaction with the side chains that influence the π-system of the Chls (Gudowska-Nowak et al., 1993; Hanson and Fajer, 1987). The consequences of such effects were observed a long time ago, in particular when the properties of Chl antenna structures from PS I were studied, and have been traditionally described as spectral heterogeneity (Gulyayev and Teten'kin, 1981; Klug et al., 1989; Kuang et al., 1984; Shiozawa et al. 1974; Thornber et al., 1979). The origin and function of long-wavelength antenna (LWA) pigments (pigments that absorb at wavelengths longer than the corresponding reaction centers) in photosynthetic antenna were studied (van Grondelle et al., 1988; Butler, 1961; Strasser and Butler, 1977). Since these spectral properties of the pigments are characteristic of the native Chl protein complex only, procedures that allow one to analyze the spectral heterogeneity and non-homogeneous broadening in the intact complexes must be developed. Finally, to describe the energy migration within antenna complexes, detailed knowledge of the chromophore-chromophore coupling strengths which determines the actual mechanism of energy transfer, i.e., coherent versus incoherent transfer or strong versus weak coupling mechanisms (Knox, 1968, 1975; Kenkre and Knox, 1974a,b; Kudzmauskas et al., 1983), is required. For almost all of the topics mentioned above, the available information is either incomplete or nonexistent. To describe the excitation dynamics in photosynthetic antenna complexes we thus have to rely to a great deal on approximations. We nevertheless think that from such simulations relevant information can be obtained that allows us to achieve a fairly detailed understanding of the various parameters that govern the excitation dynamics in antenna of higher plants and bacteria.

In this paper we concentrate on simulating the excitation dynamics of a cyanobacterial PS I antenna/reaction center complex on a molecular level by taking into account all pairwise energy transfer steps between chromophores. The aim of this work was to simulate as closely as possible the substantial amount of spectroscopic information, both steady state and time-resolved, that has been recently gathered on this antenna complex using both kinetic fluorescence as well as transient absorption spectroscopy in the picosecond time range (Holzwarth et al., 1990, 1993; Turconi et al., 1993a). We expected to gather information on a large number of hidden, i.e., not directly experimentally accessible, structural and spectroscopic parameters (Suter et al., 1987) that are important for understanding the antenna energy transfer and charge separation kinetics in the PS I particle. Based on these results, we then tried to predict the excitation wavelength and temperature dependence of the excited state kinetics in PS I particles. In addition, we also hoped to achieve a better general understanding of antenna energy migration and its relationship to structural parameters in photosynthetic antennae. The principal approximation in our approach consisted of the assumption of a completely incoherent hopping mechanism for energy transfer. This also involved the assumption of weak coupling between chromophores. Recent theoretical work has, in fact, supported such a general weak coupling mechanism for photosynthetic energy transfer in many antenna systems (Knox, 1968, 1975; Kudzmauskas et al., 1983; Pearlstein, 1982b, 1984). The simulation procedure applied in this work involves an exact solution of the Pauli master equation for excited state dynamics previously described (Suter and Holzwarth, 1987; Beauregard et al., 1991). Basically, the same procedure was used in simulations by Fleming and co-workers (Jean et al., 1989; Jia et al., 1992), although the way in which results were presented and compared with experimental data was quite different from ours.

MODEL ASSUMPTIONS

All simulations carried out in this study, unless mentioned otherwise, refer to PS I particles from the thermophilic cyanobacterium *Synechococcus* sp. The relevant experimental data from steady state and time-resolved transient absorption and fluorescence measurements and from temperature dependence of the fluorescence spectra have been reported by us recently (Holzwarth et al., 1990, 1993; Turconi et al., 1993a). For this reason, the experimental basis of the simulations in this paper are not repeated here in detail; we refer the reader to these publications. The kinetic data on PS I particles reported here are the first in which an antenna equilibration component has been kinetically resolved at higher temperature.

We used the same principal method and program for simulation as described in part 1 (Beauregard et al., 1991; see also Suter and Holzwarth, 1987). We give here only a brief description of the method and concentrate on those parts which differ from part 1. The kinetic simulation requires as input parameters the absorption and emission spectrum of each pigment, the number of pigments of each type, the spatial pigment distribution, and the pair-wise energy transfer rates between individual chromophores. To resolve the nonhomogeneous spectral broadening due to chromophore-protein interaction (both static and dynamic) we have decomposed the absorption spectrum of the isolated PS I particles into a variety of what we assume to be "homogeneously broadened" spectral Chl a forms, which are identical in spectral shape but differ in the position of their absorption maxima. Shipman et al. (1976) have decomposed the Chl a solution absorption spectrum into five Gaussian components. We have used a similar spectral shape as the homogeneously broadened basis function in our decomposition of the non-homogeneously broadened PS I absorption spectrum. However, we have assumed 10% narrower half-widths of the constituting Gaussians than given by Shipman et al., because these narrowed Chl a bands generally lead to an improved fit of the non-homogeneously broadened (experimental) PS I absorption spectrum. This (narrowed) solution Chl a basis function should be a much more realistic and meaningful representation of the homogeneously broadened Chl a spectra than the usually employed decomposition into Gaussian components (Bassi et al., 1987; Brown and Schoch, 1981). Such a non-Gaussian spectral decomposition was used recently by Trissl et al. (1993). The fitting was performed using

nonlinear least squares fitting procedures based on the IMSL tools library on a VAX computer. For calculating the corresponding fluorescence spectrum for each basis function (homogeneously broadened spectrum), the mirror image relationship (Strickler and Berg, 1962) was used, applying a Stokes shift of 110 $[cm]^{-1}$ (Shipman et al., 1976) relative to the maximum of each homogeneously broadened spectral form. This means that the reflection wavelengths had the same non-homogeneous distribution as the maxima of the homogeneously broadened spectral forms. This procedure is consistent with the assumption of diagonal disorder only. Amplitude and position of the homogeneously broadened spectral forms were generally free-running parameters. The assumed antenna size was $N = 100$ Chl corresponding to the experimental Chl/P700 ratio of 100 ± 10. A total of seven basis functions (one function was fixed in its maximum at 700 nm because of RC (P700) absorption) gave a good fit to the experimental spectrum (see Fig. 1). The relative spectral content (amplitudes) was then normalized to a total of 100 Chl a pigments, and the amplitude of each pool was rounded to the nearest integer. The results of the decomposition are shown in Table 1. This procedure can produce a maximal deviation of $\pm$ 0.5 in the number of Chls belonging to each particular pool from the best fit result. The detailed procedure for this kind of analysis will be given elsewhere (Trissl and Holzwarth, manuscript in preparation).

The RC P700 pigment is assumed to be a (monomeric) Chl species with an absorption maximum of 700 nm unless noted otherwise. It was assumed to have the same extinction coefficient and spectral shape in absorption and fluorescence as an antenna Chl.

The pair-wise rates of energy transfer k_{ij} were calculated on the basis of the Förster coupling approximation for very weak dipole-dipole-interaction (Förster, 1949, 1965). A regular square lattice (coordination number 4) with one chromophore each sitting on a lattice point was assumed for the arrangement of antenna Chls and reaction center. Alternatively a triangular lattice with coordination number 6 could have been used. Such a lattice would provide, assuming the same Chl-Chl distances, a faster energy migration. However, our results show clearly that the energy transfer times in a square lattice, at very reasonable Chl-Chl distances, are 1) very fast (judged with respect to a trap-limited kinetics) and 2) are in good agreement with recent experimental data (Du et al., 1993). We thus are convinced that the choice of two-dimensional lattice type does not represent a decisive factor for the kinetic behavior of the system (see below for comments on two- vs. three-dimensional lattices).

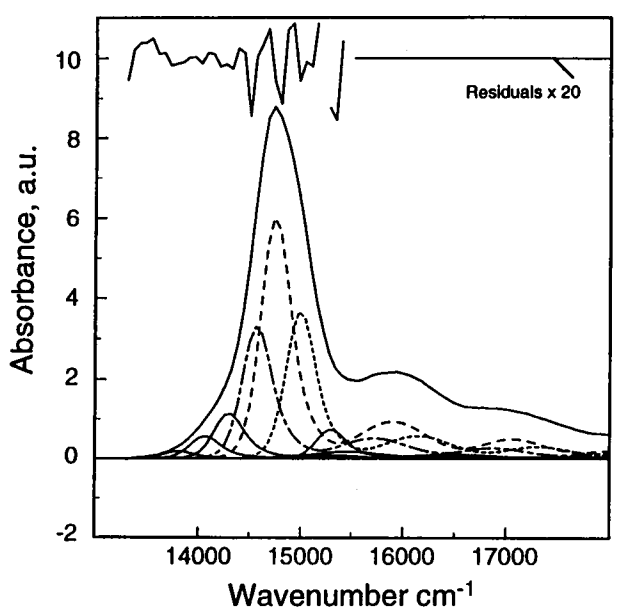

FIGURE 1 Decomposition of the absorption spectrum of the PS I particles from *Synechococcus* sp. in terms of absorption spectrum of Chl a in solution.

For the calculation of the Förster rates we used the absorption and emission spectra as described above and an average κ^2 value of 5/4 for the orientation factor, which corresponds to a random orientation of chromophores in two dimensions (Beauregard et al., 1991). Using this averaging procedure for the orientation factor, we clearly introduce some arbitrary element into the simulation. However, in view of the absence of any reliable experimental data on the actual orientation factor between Chls in the PS I antenna, we still consider this the most reasonable procedure at the present level of knowledge. Any other assumption would be even more artificial. We note, however, that any difference in the actual orientation factors from the one used here could, in the present simulation, be easily compensated (on average) by a slight adjustment in the Chl-Chl distances. Since the latter is also a fitting parameter, we think that the effect of our assumption of an average orientation factor on the final result will not be severe. In any case, the calculated pair-wise transfer rates (based on this approximation) are in agreement with recent estimates from experimental data (Du et al., 1993).

Only nearest neighbor interactions were considered for the calculation, but it was noted that taking into account non-nearest neighbor interactions does not change the results significantly. To ensure that the system relaxes to thermal equilibrium in the absence of fast excited state decay processes except energy transfer, only the downhill rate was calculated from the Förster formula, while the corresponding uphill rate constant (transfer from donors of lower energy to acceptors of higher energy) was calculated from the detailed balance relationship $k_{ji} = k_{ij}\exp(-\Delta E/T)$, where ΔE is the energy difference between spectral types i and j in units of temperature and T is a temperature. The energy transfer rates used are shown in Table 2.

Initial excitation conditions were chosen according to the extinction coefficients of the various Chl spectral types and/or the RC at the chosen excitation wavelength. For calculations of the temperature dependence of the excitation kinetics it was assumed that the spectra, and thus the calculated pair-wise downhill energy transfer rates, did not depend on temperature but only the uphill transfer rates did. Charge separation in the reaction center was explicitly taken

TABLE 1 Spectral content of *Synechococcus* sp. PSI particle model

Chl spectral type	1	2	3	4	5	6 (RC)	7	8
Absorption maximum (nm)	654.1	667.3	678.3	686.7	700	700	712.2	724
Number of Chls	5	23	38	22	6	1	4	1

TABLE 2 Energy transfer rates $k_{i\leftarrow j}$ in ps^{-1} between the Chls of spectral types *j* and *i*

i/j	1	2	3	4	5/6	7	8
1	11.6	2.61	0.35	0.09	0.03	0.01	0.00
2	12.3	12.6	4.32	1.07	0.12	0.04	0.01
3	5.76	15.1	13.5	6.81	0.86	0.12	0.04
4	3.79	9.44	17.2	14.3	3.86	0.52	0.10
5/6	4.74	4.25	9.04	16.0	15.5	5.24	0.86
7	6.15	4.71	4.54	7.65	18.4	16.7	6.28
8	5.72	6.39	4.94	4.57	9.78	20.3	18.0

The downhill energy rates were calculated according to the Förster formula (see text), uphill rates were calculated from the detailed balance relationship. Parameters used: orientational factor $\kappa^2 = 1.25$, refractive index $n = 1.3$, radiative lifetime $\tau_0 = 20$ ns, lattice constant $\alpha = 1.0$ nm, $T = 280$ K.

into account by providing an additional decay channel specific for the RC only (rate constant k_{RC} for charge separation), which leads to the formation of a radical pair. No charge recombination process was taken into account in our calculations, since so far there exists no evidence that the primary radical pair in PS I recombines back to the excited state to any significant extent (Holzwarth et al., 1993; Turconi et al., 1993a), as is the case, for example, for PS II (Schatz et al., 1987, 1988). The rates of decay without radiation from excited antenna pigments and the RC to the ground state were assumed to be 0.2 ns^{-1}.

RESULTS AND DISCUSSION

Procedures and parameter space for the simulations

Apart from the input parameters that were identical for all the simulations ("constant parameters," i.e., those described above under Model Assumptions), we have a set of "variable parameters" whose values should be optimized by comparing the results of the simulations with the experimental data. These variable parameters then contain all the information that can be obtained from the simulations. They are the following: 1) the spatial distribution of the different Chl spectral forms across the regular lattice; 2) the lattice constant **a** (distance between pigments); 3) the position of the RC in the lattice; and 4) the rate constant k_{RC} for charge separation from the RC.

For a system of $N = 100$ pigments (1 RC and 99 antenna Chls) plus a radical pair state in the RC, the solution of the Pauli master equation is represented by a sum of $N + 1$ exponentials (Beauregard et al., 1991). Their lifetimes are given by the inverse eigenvalues of the Pauli master equation and the amplitudes are given by a bilinear form of the eigenvector components weighted by the initial conditions (see Beauregard et al., 1991, for further details). This is a convenient property of these simulations since in principle both the eigenvalues and the amplitudes (often represented as decay-associated spectra (DAS), i.e., amplitudes as a function of emission wavelength) are experimentally accessible quantities in lifetime measurements (Suter and Holzwarth, 1987; Holzwarth et al., 1987; Roelofs et al., 1992). In practice, limitations exist and only a limited number of eigenvalues and DAS can be resolved experimentally. First of all, most of the DAS from the simulations have very small magnitude, which means that they are of no practical interest. Thus when comparing the simulations to experimental data only the largest DAS are relevant. Likewise, we are most interested in those DAS that have the smallest eigenvalues, e.g., those with lifetimes above a certain value (for our purposes, the lower limit is about 0.2 ps). Even with these restrictions, however, the number of predicted eigenvalues from the simulations is generally still too large for a direct comparison with the available experimental data. Furthermore, we need to consider aspects of the principal practical experimental resolvability of multi-exponential component kinetics. Thus, to further reduce the number of simulated lifetime components to a reasonably small number, we performed a remapping of the calculated exact solution of eigenvalues and DAS to a smaller set: close-lying eigenvalues were averaged to form groups with average value ϵ_{av} to cover a range $\epsilon_{av} \pm 30\%$. For the eigenvalues falling into such a range, the corresponding DAS were also averaged. The results presented thus are generally averaged eigenvalues and DAS, which should be close to what is actually measured in a lifetime experiment. We did not apply this averaging to the two or three smallest eigenvalues, which are almost always presented in their pure non-averaged form with their pure corresponding DAS. In some cases, the resulting averaged eigenvalues might still be too closely spaced to be resolved experimentally. However, this is a more practical experimental problem rather than a fundamental one. Its solution in each case depends on the details of the measurement, i.e., its signal/noise ratio, the detection method and data analysis used, etc. Generally speaking, for the results presented here (in comparison with available experimental data) no substantial problems arise in this respect. The problems will become more severe, however, if higher time resolution is to be achieved in the future, since more components with close-lying lifetimes (eigenvalues) will arise. We are convinced, however, that the approach chosen here is useful and more informative than a reanalysis of convoluted simulated lifetime data as performed in the work of Jia et al. (1992).

Simulations for temperature 280 K and excitation wavelength $\lambda_{exc} = 670$ nm

The most extensive set of experimental data for this PS I particle is available for a temperature of 6°C and an exci-

tation wavelength of 670 nm. For this reason, we performed most simulations first for that temperature and excitation wavelength. The PS I particle from *Synechococcus* sp. has an antenna size of about 100 Chl/P700 (Turconi et al., 1993a). We thus for all simulations chose a regular two-dimensional 10×10 square lattice as the principal spatial arrangement of antenna Chls and RC. As the direct results of the simulations, we obtain the steady-state fluorescence spectrum, the lifetimes and corresponding decay-associated spectra of each lifetime component, the charge separation yield, and the time dependence of the population of each species for each chosen spatial arrangement of antenna chromophores and RC. These output data can be compared with experimental results, which provides a feedback for changes in the adaptable parameters of the model. The experimental data from the PS I particle from *Synechococcus* sp. that we tried to reproduce by these simulations are the following (Holzwarth et al., 1990, 1993; Turconi et al., 1993a):

1) An energy equilibration time of ~12 ps between the main pool of antenna pigments and some LWA pigments with absorption and emission maxima ~710–725 nm.

2) The correct shape of the corresponding DAS to the 12-ps component which shows a positive amplitude maximum around 690 nm and a negative amplitude maximum (rise term) at ~720 nm with a zero-crossing wavelength at 711 nm.

3) The overall charge separation time of ~35 ps and its DAS with a pronounced shoulder at 690 nm and a maximum at 720 nm.

4) The steady-state emission spectrum of the PS I particle with a shoulder at 690 nm and a maximum at 720 nm.

5) We also tried to reproduce an ultrafast equilibration component with a lifetime of ~1–2 ps, which seems to correspond to equilibration of main pool pigments (absorbing around 675 nm) and pigments absorbing around 700 nm (Holzwarth et al., 1993).

From previous model simulations, we expect that in particular the components with negative amplitudes (rise terms) are sensitive indicators of the pigment structural arrangement in the antenna (Beauregard et al., 1991).

The simulations to be performed in principle represent a nonlinear fitting problem to a set of experimental data. However, several important difficulties arise. First, the problem is under-determined by the insufficiently resolved experimental data. Thus no exact and/or unique solution exists. It will thus be the aim of the simulations to search as large a parameter space as possible and to choose such solutions that best reproduce the available experimental data. A second problem arises in that the pigment distribution over the lattice represents a noncontinuous (discrete) set of variables. However, for a total lattice size of 100 pigments consisting of 8 (7 spectral types and 1 RC) types, the parameter space is huge and we can never expect to sample all the possibilities. For all these reasons, conventional nonlinear fitting techniques are unsuitable to find a solution. However, after some experience with the simulations, one realizes that the actual number of parameters on which the results do react sensitively are relatively few. The critical parameters are the absolute and the relative location of the RC and the LWA pigments on the lattice, the rate constant k_{RC}, and the lattice constant **a** (the pigment spacing). After a series of initial test runs we thus chose the following strategy to find the desired parameters. We started off with six fundamentally different pigment distributions in the lattice: 1) monomeric (M), characterized by avoiding as much as possible the neighborhood of pigments of the same spectral type; 2) dimeric (D), containing dimers, i.e., two pigments of the same type next to each other but surrounded by pairs of another spectral type; 3) trimeric (T), containing trimer arrangements according to the same rules as for dimeric; 4) tetrameric (Q), arrangement of identical pigments; 5) random (R), arrangements generated by a random number generator; 6) funnel (F), arrangement with pigments arranged such that the longest-wavelength absorbing pigments are closest to the RC and excited state energy increases with increasing distance from the RC. See Fig. 2, where lattice patterns obtained after optimization are presented, for the basic features of these arrangements.

For all these arrangements the initial RC location was near the center of the 10×10 square lattice (position 5,5). Within these fundamental patterns we varied the pigment locations, in particular the position of the LWA pigments to each other and to the RC, in a systematic manner. The main search criterion during this stage was the shape and the relative magnitude of the DAS of the two or three smallest eigenvalues. This procedure was carried out until these DAS reproduced the experimental DAS well, even if their lifetimes (inverse eigenvalues) were substantially in error. Once a good pigment arrangement was found according to these criteria, we rescaled the lattice constant **a** and the rate constant k_{RC} from their starting values. This rescaling is based on the following observations and relationships. Since rescaling the lattice constant **a** rescales all pair-wise energy transfer rates, basically all eigenvalues rescale accordingly. Keeping the pigment distribution constant in this way, the eigenvalues (mainly the second and third smallest eigenvalues were considered) representing energy transfer were scaled to fit the experimental values well. This scaling procedure did not significantly change the corresponding DAS. Second, we rescaled k_{RC} which, as actually expected, affects almost exclusively the smallest eigenvalue, which in all cases is representative of the overall charge separation rate constant. Thus the calculated overall charge separation rate was brought to coincide with the corresponding experimental lifetime, which has been shown to be due to charge separation (Holzwarth et al., 1993; Turconi et al., 1993a). The lifetimes τ_1 before the rescaling procedure are given in Table 3. After further adjustment of pigment distributions and rate constants in a second or third round analogous to the procedure described above, the simulation was stopped. First passage times were calculated in each case by choosing for the charge separation rate constant k_{RC} a high value (10^3

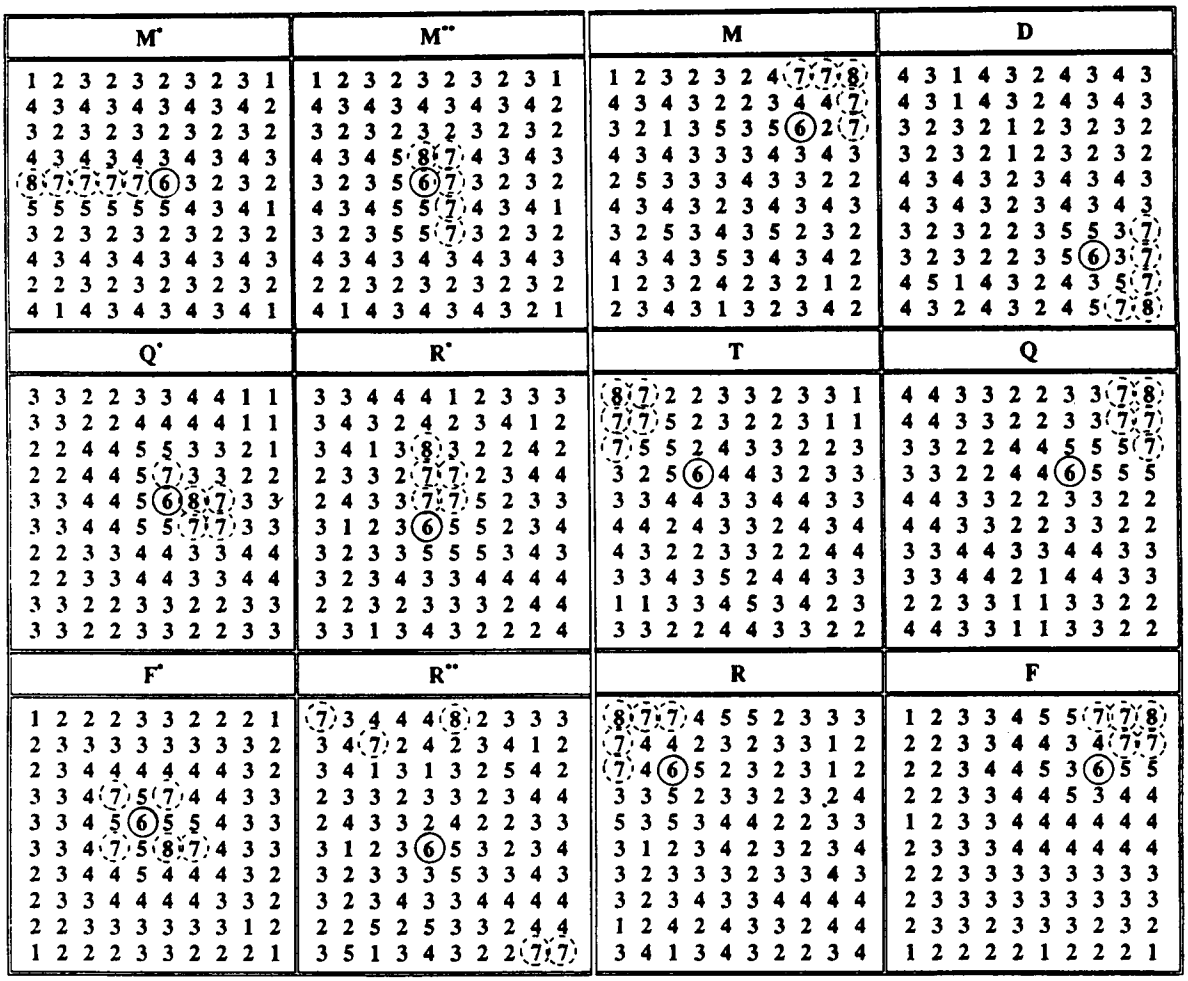

FIGURE 2 Pigment lattice arrangements as described in the text. Capital letters indicate the original pigment distribution. Numbers indicate the spectral type of Chl molecule (see Table 1).

TABLE 3 Optimized values of lattice constant a and RC trapping rate k_{RC} for the pigment arrangement patterns presented in Fig. 2

Pattern	a (nm)	k_{RC} (ps^{-1})	τ_1 (ps)	τ_2 (ps)	FPT (ps)
M	1.14	2.3	144	7.0	19.1
M*	1.54	3.	161†	18.6; 15.0†	18.9
M**	1.08	2.5	148†	11.4†	18.9
D	1.09	2.5	145	7.2	16.5
T	1.19	2.	141	4.1	14.4
Q	1.17	1.7	138	4.8	12.9
Q*	1.56	2.5	149†	10.1; 9.4†	19.9
R	1.11	2.	142	6.3	16.4
R*	1.44	2.2	153†	18.9; 16.5†	19.5
R**	1.04	10.	158	14.5	38.0
F	1.14	4.	139	1.5	27.0
F*	1.73	10.	148†	5.4; 4.3†	30.4

The lifetimes τ_1 and τ_2 before rescaling as well as the first passage time FPT are also given in the last three columns (initial values of the lattice constant **a** = 1.0 nm (**a** = 1.5 nm)† and k_{RC} = 0.3 ps^{1}), for details see text. The two lifetimes appearing in the column τ_2 represent the lifetimes of the DAS that were summed up.

ps^{-1}). The average rise time of the radical pair in this case represents the first passage time (Beauregard et al., 1991).

Simulations were performed starting with the lattice distances **a** of 1.0 nm or 1.5 nm. The latter value was estimated from PS I particle volume (Boettcher et al., 1992) and probably represents an upper limit of the true lattice distance. Still larger values would give rise to excessively long average migration times to the RC (first passage times). The former value of **a** is typical of average pigment distances found recently in the crystal structures of both LHC 2 from higher

plants (Kühlbrandt and Wang, 1991) and for PS I particles from *Synechococcus* sp. (Krauss et al., 1993). Initial values for the trapping rate constant from the RC were $k_{RC} = 0.3$ ps^{-1} as suggested by Owens et al. (1987).

In the course of the simulations starting with **a** = 1.5 nm we found that the DAS and lifetimes are highly sensitive to the pigment arrangement. For all of the basic lattice arrangements mentioned above it was found that the most sensitive factor was the mutual arrangement of the LWA pigments relative to each other and to the RC. Spreading the LWA pigments more or less homogeneously across the lattice, we obtained very long (up to 200 ps) τ_1 values before rescaling (lifetime values will be arranged by decreasing lifetime; in general, the τ_1 lifetime represents the overall charge separation, while τ_2 to τ_n represent energy transfer components within the antenna). The longest energy transfer component τ_2 had rather large values as compared to the experimental one (about 12 ps), and the corresponding DAS was much too small in amplitude. For the M** and R* pigment arrangements (c.f. Fig. 2) the DAS obtained after final rescaling are presented in Fig. 3. The DAS of the τ_1 component of both patterns has too high a shoulder at 690 nm, and the crossing point of the DAS of the τ_2 component is not located at the proper wavelength. The positive τ_2 amplitudes are too low as compared with the experimental ones. More reasonable DAS were obtained only after the LWA pigments were collected into one pool ("red aggregate," RA) and positioned close to the RC. However, only three pigment arrangements were found to be reasonable in reproducing the experimental DAS (c.f. the optimized patterns M*, Q* and F* in Fig. 2 with the optimized **a** and k_{RC} values in Table 3). Among these lattice patterns one can see two distinct types of RA organization. In the pattern M*, which represents a more or less homogeneous distribution of spectral forms, lattice type 8 Chl is placed on the edge of the lattice and type 5 as well as type 7 Chls form the channel for the fast energy transfer from the type 8 Chl to the RC. In the other two patterns actually showing highly "aggregated" LWA Chls, red pigments were placed around the RC with type 8 Chl being either the nearest (Q*) or the next to nearest neighbor (F*).

For all the different patterns, a lattice constant of 1.5 nm gave rise to excessively long energy transfer and overall charge separation lifetimes, and the excited state distributions reached Boltzmann equilibrium only at very long times (>100 ps). This was evidenced also in the calculated steady-state fluorescence spectra (Fig. 4), which were far from the experimental ones and also far from the theoretically calculated Boltzmann-equilibrated spectrum. No improvement in the situation was possible by choosing different pigment arrangements.

Further calculations were carried out with a lattice constant of 1.0 nm. For LWA pigments spread over the whole lattice, the DAS looked quite similar to those obtained for lattice constant 1.5 nm; however, in many cases, the lifetimes were much improved. For pigment arrangement R**, no reasonable values were obtained. The first-passage time of 38 ps, as well as the lifetimes and the shapes of the DAS (Fig. 5), indicated that this kind of pigment distribution can be excluded when compared with the experimental data (Holzwarth et al., 1993). Again the LWA pigments were grouped

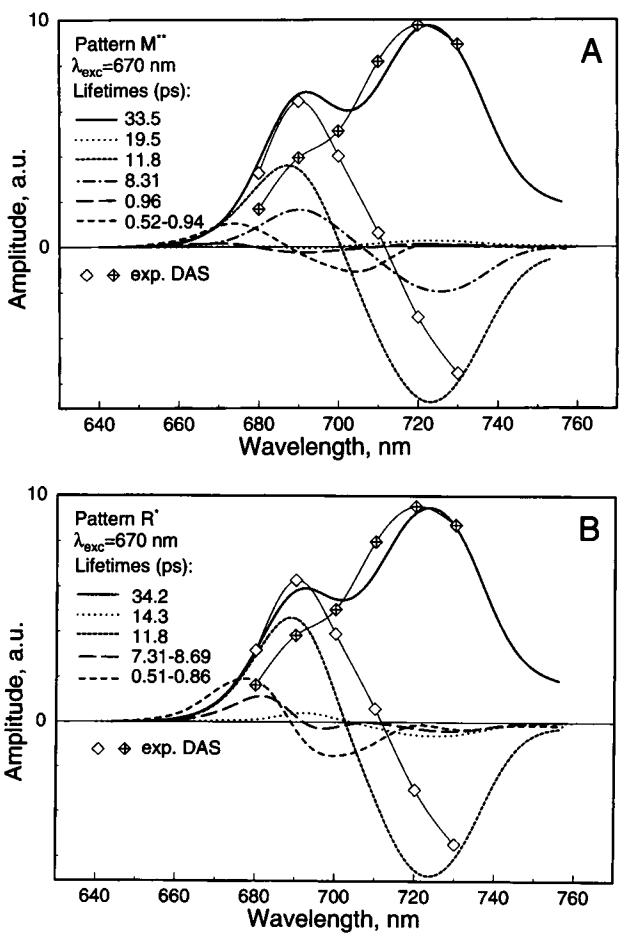

FIGURE 3 DAS obtained after final lifetime rescaling. (*A*) M**, (*B*) R* pigment arrangements, respectively. The initial value of the lattice constant **a** = 1.5 nm.

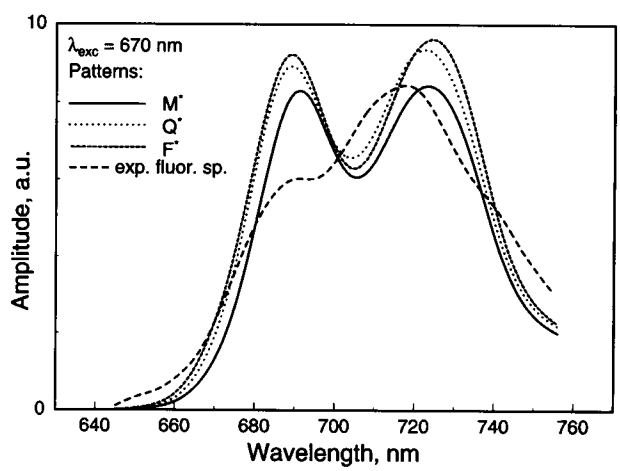

FIGURE 4 Steady-state fluorescence spectra for the lattice arrangements M*, Q*, and F* optimized upon starting with **a** = 1.5 nm. *Dashed curve*: experimental fluorescence spectrum.

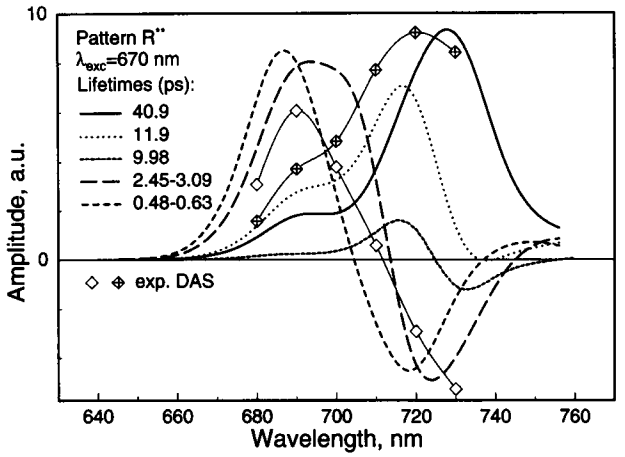

FIGURE 5 DAS obtained after final lifetimes rescaling for the pigment arrangement R**. The initial value **a** = 1.0 nm.

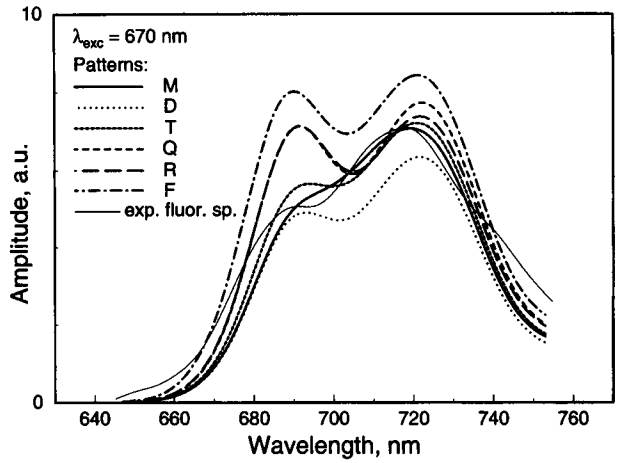

FIGURE 6 Steady-state fluorescence spectra for M, D, T, Q, R, and F lattice arrangements obtained starting with **a** = 1.0 nm. *Thin line:* the experimental fluorescence spectrum. For the final parameter values of **a** and k_{RC}, see Table 3.

into a RA complex, which improved the situation substantially. Results even closer to the experimental data were obtained when the RA was moved to the corner of the lattice and the RC was placed nearby the RA complex, i.e., off the center of the lattice, but not in direct contact with the RA complex (see arrangement M in Fig. 2). With increasing RC–RA distance the charge separation lifetime τ_1 was constantly growing. The τ_2 lifetime depended strongly on the RA local environment. The pigments surrounding the RA complex form an energy funnel for the exciton flow from the main pool to the RA complex. Properly choosing the energetic slope and structure of this funnel proved essential to obtain the proper τ_2 lifetimes and DAS. Surrounding pigments with a less steep funnel than the optimal one led to too small a lifetime τ_2 and a low positive amplitude of the corresponding DAS. Too large an energetic slope of the funnel resulted in too high a positive amplitude of the τ_2 DAS. The local environment of the RC had to be chosen such that the RC provided a shallow trap to its immediate surrounding pigments (ratio of detrapping to trapping rate ~0.45, taking into account all four neighbors). This general local environment as well as the relative RA–RC arrangement was found to be best for all six basic pigment distributions. For all arrangements a few (up to 10) short lifetime components in the range of 0.5–5 ps with substantial magnitude of their DAS were obtained. Their exact shape and lifetimes depended strongly on the exact details of the pigment arrangement. This indicates that experimental data for higher time resolution than those are available now would contain much more structural information.

The calculated steady-state fluorescence spectra for all of the various optimized lattice patterns (see patterns M, D, T, Q, R, and F in Fig. 2 and the optimal rescaled parameters **a** and k_{RC} in Table 3) were more or less deformed at the blue side of the spectrum, which indicates relatively slow thermal equilibration between the RA and the main pigment pool (see Fig. 6 and Discussion below). The best results of all six basic arrangements were obtained starting from the monomeric

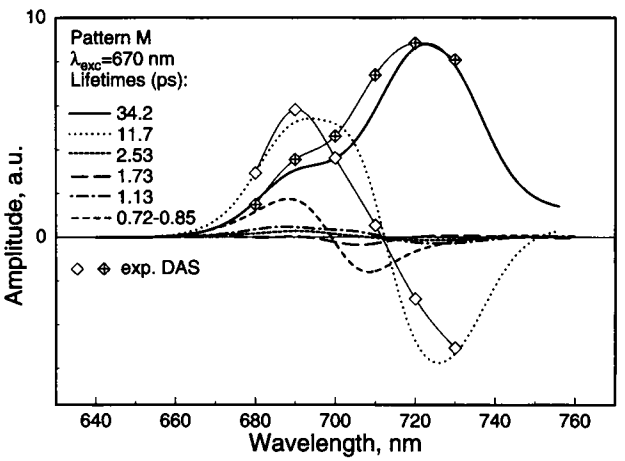

FIGURE 7 DAS for the lattice arrangement M obtained starting with **a** = 1.0 nm at T = 280 K.

pigment distribution M (Fig. 2). The calculated DAS for τ_1 and τ_2 and their corresponding lifetimes (c.f. Fig. 7) and the steady-state fluorescence spectrum (Fig. 8) reproduced the experimental data well. Furthermore, the predicted 0.8-ps component (τ_6) and its DAS show features quite consistent with the preliminary transient absorption data at time t = 0 after the excitation pulse as well (Holzwarth et al., 1993). Thus the results of the optimized simulations on pigment arrangement M (Fig. 2) are well suited to explain the experimental findings. The main pigment pool consists of pigment types 1 to 4 and a small number of longer wavelength pigments (type 5) embedded in that pool, which serve as local exciton traps. Excitation equilibration within this main pool is very rapid and gives rise mostly to lifetimes up to about 2 or 3 ps. In the lattice arrangement M, the lifetime τ_2 is almost exclusively related to the transfer of excitation from the main pool to the RA of LWA pigments. This follows from Fig. 9*A*, which shows the time dependence of the populations

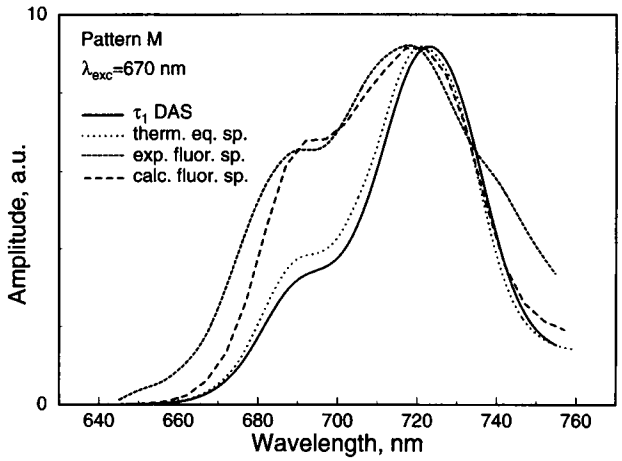

FIGURE 8 Comparison of the calculated τ_1 DAS, the thermally equilibrated fluorescence spectrum, and the experimental and the calculated steady-state fluorescence spectra.

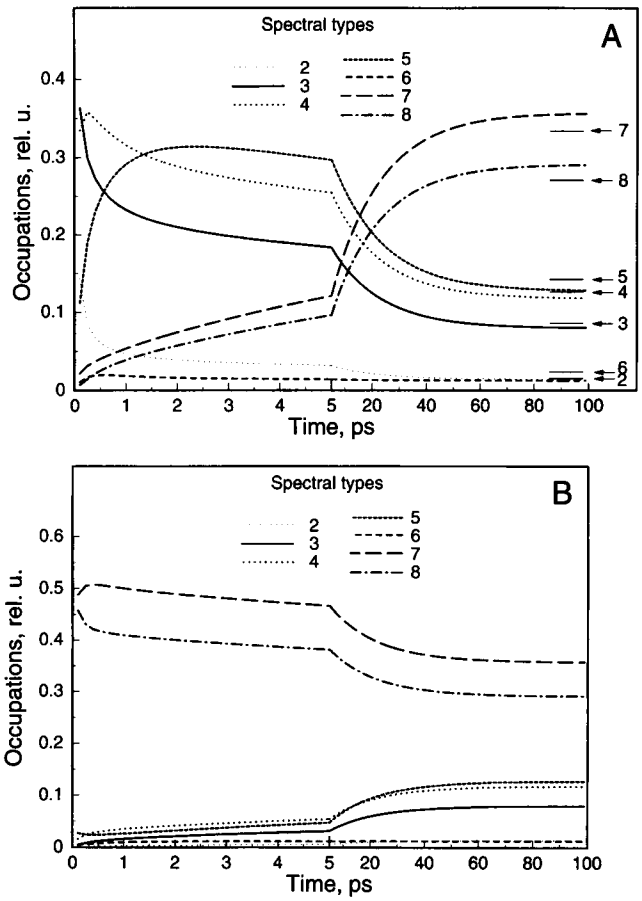

FIGURE 9 Time dependence of the decays of the total excited state occupations of the spectral type Chls molecules (c.f. Table 1) normalized to the total excited state concentration. (*A*) λ_{exc} = 670 nm; (*B*) λ_{exc} = 725 nm. The arrows indicate corresponding occupations as predicted by Boltzmann distribution (*thin lines*). The occupations of spectral type 1 are not shown because of their very low values.

of the different pigment types. It follows from that figure that basically all pigment types except for the RA pigments (types 7 and 8) reach a concentration close to Boltzmann equilibrium in only a few picoseconds. It is interesting that, at long times, the RA pigments reach an excited state concentration that is above the Boltzmann concentration. A detailed analysis of the DAS and eigenvalues reveals that this is explained by the fact that the return rate from the RA pool to the main pool or to the RC is slower than the decay of the main pool due to charge separation. This is also indicated by Fig. 9 *B*, which shows the time dependence of excited state concentrations when initially only type 8 Chl was excited (λ_{exc} = 725 nm). Under such conditions the main pigment pool (except for type 5 Chls) is equilibrated again within a few picoseconds, while equilibration with type 5 as well as RA pool pigments takes up to 40 ps (about 3 times τ_2). This means that the RA pool in our simulations is not in full equilibrium with the main pigment pool at long times during the process of exciton trapping by the RC. This is also shown by the calculated steady-state fluorescence spectrum for lattice arrangement M (see Fig. 8). We have tried to improve this situation in the simulations by choosing a more favorable arrangement of pigments to funnel energy more quickly between the main pool and the RA pool and vice versa. All such attempts led to a considerable change in the positive amplitudes of the τ_2 DAS component, such that deviations from the experimental ones were quite pronounced. We could not find a pigment arrangement that would afford a more complete equilibration of RA pool with the main pool. Thus, within the chosen model, some deviation from Boltzmann equilibrium for the RA pool remains. It is difficult to judge at the present level of experimental data available whether this is true for the real PS I system as well. It might be an interesting finding from these simulations to understand the reasons for possible incomplete equilibration. It might well be, however, that our model predicts the wrong kinetics in this respect. Failure of our model might have a number of different reasons. First, we could have missed the proper pigment arrangement that gives rise to more complete equilibration. This possibility cannot be excluded in view of the very large number of possible arrangements. Nevertheless, this possibility is considered to be unlikely, in view of the many arrangements we tested. It is more likely, in our view, that some of the basic assumptions in our model could be inappropriate for a real photosystem. In principle, any of the model assumptions could be wrong. However, in view of the otherwise encouraging results, we think that at the present level of approximation, one severe limitation of our model is the restriction to a two-dimensional system. In a three-dimensional lattice, equilibration could occur considerably faster (Montroll, 1969). Recent x ray data indicate clearly that the real pigment arrangement is three-dimensional rather than two-dimensional, although some structural restrictions that may cause the topography for energy transfer of the PS I system to become quasi-two-dimensional (Krauss et al., 1993; Boettcher et al., 1992) may apply. Therefore, for the next level of simulation we will have to use a three-dimensional lattice for the pigment arrangement.

Overall the data indicate a hierarchy of several energy transfer processes in PS I. A very fast exchange among small

groups of short-wavelength-absorbing pigments gives rise to a variety of very fast lifetime components (ranging from 0.1 ps to ~0.7 ps). Such sub-picosecond lifetimes have been reported recently by Du et al. (1993). This is accompanied by a slower energy transfer process of about 0.8 ps, which equilibrates larger groups of pigments (donor type 5 and acceptor types 2, 3, and 4). This latter process probably gives rise to the rapid (1–2 ps) excited state redistribution seen in our transient absorption data (Holzwarth et al., 1993) as well as in the work of Causgrove et al. (1988). On a significantly slower time scale (τ_2 = 12 ps), the main pool transfers energy to the pigments of the RA complex. This latter step gives rise to the characteristic positive/negative going DAS found in all of our kinetic fluorescence measurements (Holzwarth et al., 1993; Turconi et al., 1993b).

Charge separation rate k_{RC}

The optimized parameter sets in our simulation require that we increase the charge separation rate k_{RC} from the initial starting value of 0.3 ps^{-1} to a value of ~2.3 ps^{-1}, i.e., by nearly an order of magnitude. We consider this to be too high a value for the primary charge separation rate. If the value were correct, k_{RC} for PS I would be much faster than the corresponding values known from bacterial RCs (2.8 ps) (Parson, 1991) and PS II (~3 ps) (Wasielewski et al., 1989; Schatz et al., 1988; Roelofs et al., 1991). Further consideration reveals that calculations of the first passage time carried out in the way as described above indicate that it contributes ~50% to the overall charge separation time τ_1 under our conditions (Table 3). This means that energy transfer in our model is probably still too slow. If energy transfer were much faster, this would allow the rate constant k_{RC} to be decreased by maximally a factor of 2, still substantially higher than known values for RCs. However, the problem cannot be solved by decreasing the lattice constant **a**, since then we would lose the proper values of other lifetimes in particular the equilibration component. One resolution of this problem might be to choose two different lattice constants, i.e., one for the LWA pigments and another smaller one for the main pool pigments and the RC. We have not tested such models in detail, since we think that other factors play a more essential role and should be optimized first. The two most important ones are the following. First, there are indications (Golbeck, 1993) that the primary donor of PS I may be a Chl dimer, as in the other known RC complexes. If this is the case, it could possibly increase the overall charge separation rate due to a larger exciton capture cross-section (one could, for example, simulate this within our model by distributing the RC over two lattice sites). Furthermore, if charge separation could be allowed to occur from both sites occupied by the RC, then one could reduce the rate constant k_{RC} by about a factor of 2 without changing the energy transfer lifetimes. The second important factor is the topography of the PS I antenna, which we assume to be two-dimensional. Choosing a three-dimensional pigment arrangement would reduce the first-passage time in the antenna array (Montroll, 1969; Pearlstein, 1982a) without increasing the pair-wise transfer rates. The rate constant k_{RC} could again be decreased. Furthermore, a refinement of the spectral properties of P700, which are not well known, could result in increased pair-wise energy transfer rates to the RC and thus could add also in the same direction resulting in a final decrease in k_{RC}. All of these effects could be large enough to finally allow k_{RC} to be ≤ 1 ps^{-1}, which would be a more reasonable range.

Simulations of excitation wavelength dependence of the kinetics

Calculations of the excitation wavelength dependence were carried out using the optimized pigment arrangement, lattice constant and charge separation rate values, etc. for lattice M that best reproduced the experimental data within our model (Fig. 7). Note that the eigenvalues of the system will be independent of the excitation wavelength and only the DAS will respond to a change in excitation wavelength. The results of four additional excitation wavelengths are shown in Fig. 10.

The data obtained indicate the existence of characteristic time scales of the excitation energy exchange among the pigments of different spectrum. Excitation at 685 nm (Fig. 10 *A*) has no significant influence on the DAS except some negligible reduction of all the amplitudes due to direct excitation to a small extent of type 5 as well as RA pigments. Excitation at 695 nm (Fig. 10 *B*), i.e., close to the wavelength at which the τ_6 (~0.8 ps) DAS changes sign, resulted in significantly reduced τ_6 DAS amplitudes. This means that the excited state population of the main lattice pool as well as the type 5 pigments just after the excitation were close to equilibrium. The τ_6 DAS after excitation at 705 nm (Fig. 10 *C*), i.e., exciting mostly type 5 pigments, inverted its sign, thus indicating reverse excitation energy flow from type 5 pigments to the main pigment pool. (Note the negative DAS amplitude below 700 nm and the fact that the 2.53-ps component vanished). The same effect has been observed in the τ_2 DAS when the excitation wavelength was increased to 715 nm (Fig. 10 *D*). In this case, the main pigment pool was supplied with excitation energy from the RA. When excitation of about 710 nm wavelength is applied, the τ_2 DAS vanishes, indicating approximate equilibrium energy distribution between the RA and the main pool pigments after excitation. We conclude from these data that experimental excitation wavelength studies will contain a substantial amount of information about the spectral heterogeneity and pigment organization.

Prediction of temperature dependence

For simulation of temperature dependence, we again used the optimized pigment distribution pattern M as described above (Fig. 2). The spectra of the pigments were assumed to be temperature-independent. This means that also the pair-wise downhill energy transfer rates were temperature-independent. Because of the detailed balance relation condition for

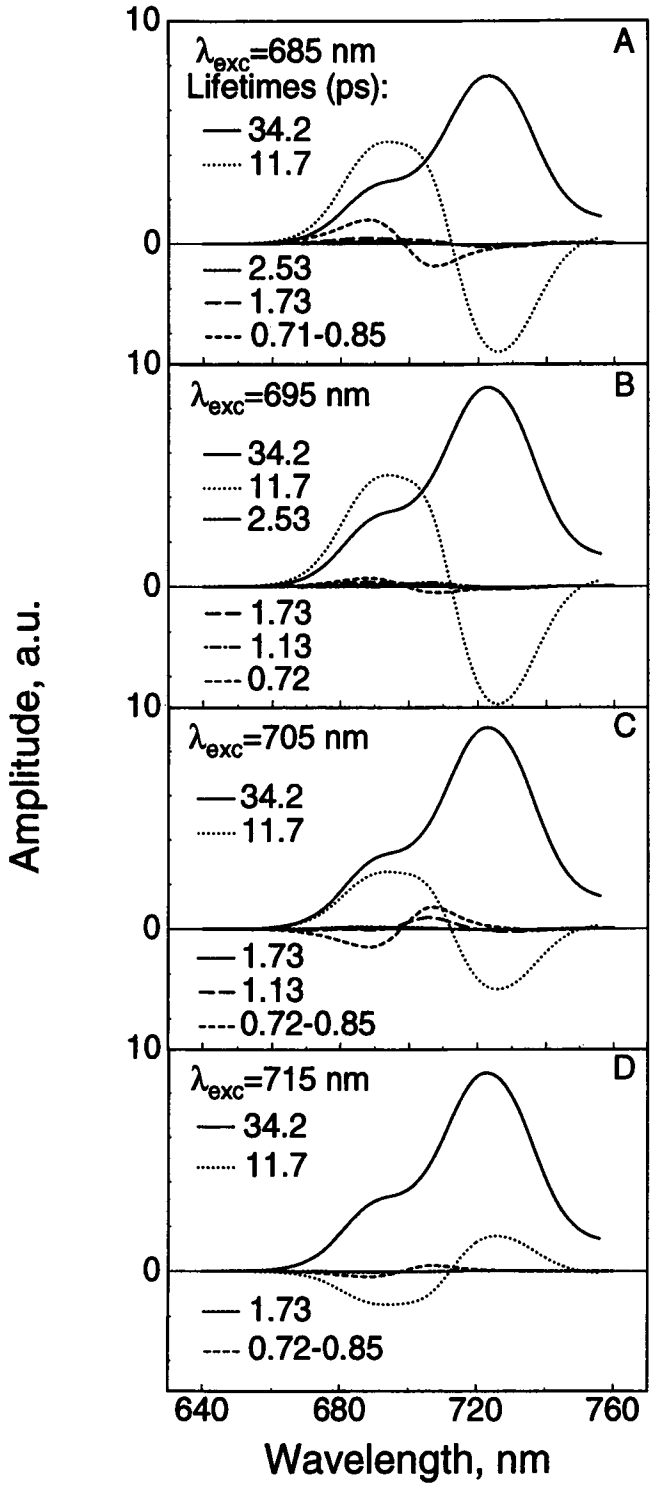

FIGURE 10 Calculated DAS dependence on the excitation wavelength λ_{exc} = (*A*) 685 nm; (*B*)- 695 nm; (*C*) 705 nm; (*D*) 715 nm.

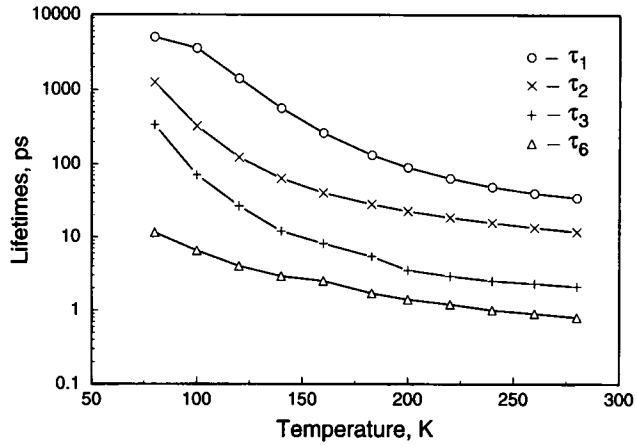

FIGURE 11 Temperature dependence of first three longest and one shorter lifetimes (the latter being ~0.8 ps with significant amplitude at 280 K; see Fig. 7).

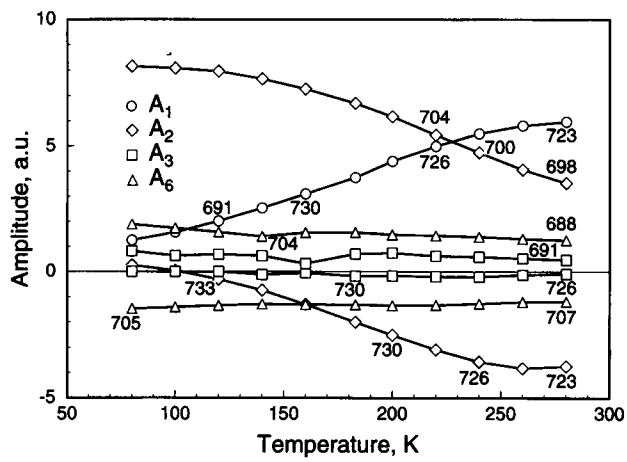

FIGURE 12 Temperature dependence of the minima/maxima of the DAS amplitudes for the first four lifetimes. The wavelengths of the amplitude maxima/minima are indicated by the numbers near the points (these are the same for the points to the left).

uphill transfer, however, the pair-wise uphill transfer rate constant was temperature-dependent. Calculations were carried out for an excitation wavelength of 670 nm. Figs. 11 and 12 show the temperature dependence of the three longest lifetimes as well as the ~0.8-ps component and their corresponding DAS amplitudes (values taken at their respective maximum wavelengths). Fig. 13 shows the calculated steady-state fluorescence spectra for a range of temperatures from 280 to 80 K. Comparison of these simulated data with experimental steady-state and time-resolved data (c.f. Turconi et al., 1993a, and unpublished observations) indicates that, in general, the simulations predict reasonable kinetics and spectra down to a temperature of about 150 K within a factor of 2 in lifetimes. The two longest lifetimes are too long as compared with experimental ones. Below ~120 K, a steady-state emission band at ~705 nm starts to rise strongly and becomes the dominant emission peak at 80 K. This does not agree with the experimental findings (Turconi and Holzwarth, unpublished observations). It can be seen from the simulations that this strong deviation from the experimental spectrum at low temperatures arises, to a large degree, from local trapping on the four type 5 pigments, which are distributed within the main pigment pool, in the arrangement M.

There are several reasons why simulated and experimental data at lower temperatures might deviate. First, it is possible

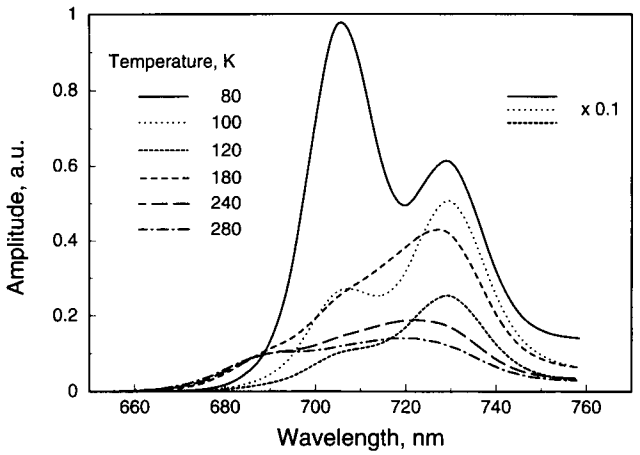

FIGURE 13 The predicted steady-state fluorescence spectra at various temperatures. Spectra at 80, 100, and 120 K are reduced by a factor of 10.

that we have not chosen the location of these pigments properly at 280 K. However, this possibility is unlikely, since the necessary changes in the pigment distribution were very limited at 280 K in order to describe the experimental high temperature data well. One way to solve this problem would be to decompose the spectrum into more than 7 spectral types, such that the energy difference between the Chl spectral types would become smaller. The relatively large energy gap, even between some of the energetically neighboring pigment types, leads to a steep decrease in transfer rates with decreasing temperature and thus to fairly long first passage times at low temperatures. Taking into account next to nearest-neighbor interactions might also help to some extent. Second, we cannot ignore entirely the temperature dependence of absorption spectra and also the possible change of non-homogeneous broadening with temperature. Recent calculations of the Chl absorption spectral shapes as a function of temperature indicated only a modest temperature dependence (Jia et al., 1992), which nevertheless could lead to changes in pair-wise rate constants in the order of a factor of 5. However, even such changes in rate constants are not sufficient to reverse the large deviations in our low temperature simulations. A third factor that could lead to an incorrect prediction of the temperature dependence is again the two-dimensional nature of our lattice. Switching to a three-dimensional lattice might help to overcome this problem. In the following we will thus only discuss data for temperatures above 150 K.

The simulations correctly predict a strong increase in fluorescence around 730 nm when lowering the temperature below 280 K. The band at 690 nm almost disappears at low temperature, concomitant with the appearance of a shoulder near 705 nm. This event has been reported experimentally (Turconi et al., 1993a). The four lifetimes under consideration increase more or less in parallel and monotonically with decreasing temperature to give rise to a τ_1 lifetime of 130 ps at ~180 K, which should be compared with an experimental value of 72 ps (Turconi et al., 1993a). These changes are paralleled by a modest increase in the amplitude of the longest lifetime component τ_1 at long wavelengths and a decrease at short wavelengths. This behavior was actually expected from the detailed analysis of the simulation data at 280 K. Substantial changes occur in the shape of the τ_2 component DAS. Its zero crossing wavelength moves to longer wavelengths with decreasing temperature. Changes in the amplitudes of the other lifetime components are predicted to be less pronounced. Temperature decrease is accompanied with a pronounced increase in the first passage time of the pigment array. Thus the tendency to a more diffusion-limited kinetics at low temperature is indicated, which is not unexpected.

Calculations with reduced numbers of LWA pigments

The likely location of the RA at the corner of the lattice might lead to loss of the LWA pigments during biochemical isolation procedures, depending on detergent. Evidence for such LWA loss is found in the literature (Werst et al., 1992). To simulate the effect of the loss of the LWA pigments on the exciton decay kinetics, we performed calculations for the optimized pigment arrangement M with fixed scaling parameters but removing from the lattice successively 1) type 8 Chl, 2) two type 7 Chls, and 3) all the RA pigments.

The lifetimes as well as their DAS obtained in case 1 are shown in Fig. 14 *A*. The loss of the single type 8 Chl resulted in our simulations in the reduction of the two longest lifetimes τ_1 and τ_2 by about 30%. The amplitudes of the τ_2 DAS were reduced by 30–50%, while the steady-state fluorescence spectrum showed minor effects only of the RA content change. The τ_2 DAS maximum as well as minimum were blue-shifted by about 5 nm. Dramatic changes were obtained when removing in addition two type 7 Chls. As one can see in Fig. 14 *B* for all the wavelengths below 710 nm, the exciton decay is nearly single-exponential with a lifetime of 21 ps (not taking into account the unchanged ~0.8 ps component). The τ_1 DAS maximum gets blue-shifted further by 10 nm, while the τ_2 DAS minimum wavelength remained the same as in case 1. The shape of the steady-state fluorescence spectrum now became similar to the τ_1 DAS. As was expected, when all the RA pigments were removed, the exciton decay kinetics lost the component τ_2 (Fig. 14 *C*). The τ_1 DAS and the steady-state fluorescence spectrum narrowed and showed a broad maximum in the range of 690–705 nm. The lowering of the temperature had no strong influence on the decay time as was observed for pattern M (c.f. Fig. 11). Lowering the temperature from room temperature to 183 K, τ_1 increased from 18.8 ps to 30 ps (compare with the corresponding change from 34 ps to 132 ps for pattern M) and the effect was apparent even if type 5 Chls were near the RC instead of being spread over the lattice.

Our data on the lattices with reduced LWA pigments are in line with the kinetic data of the mutant strain of *Chlamydomonas reinhardtii* A4d (Jia et al., 1992; Werst et al., 1992), which showed no rising kinetic components and only small lifetime changes upon temperature variation. Our simulations seem to indicate that the PS I of the mutant whole

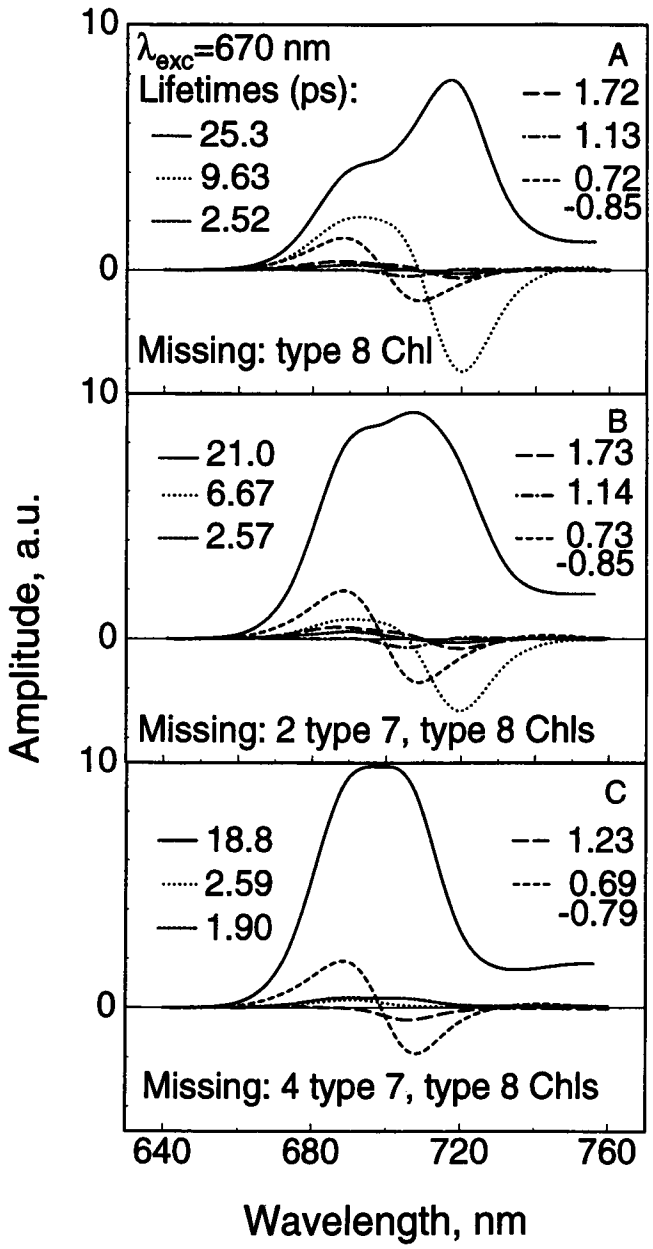

FIGURE 14 DAS calculated for the optimal lattice pigment arrangement M and optimized parameters but missing the LWA Chls. (*A*) minus type 8 Chl; (*B*) minus type 8 and two type 7 Chls; (*C*) missing all LWA pigment types 7 and 8.

cells as well as the PS I core particles used in the work of Werst et al. (1992) were probably lacking most of the LWA pigments. This would explain the lack of pronounced rising components in the fluorescence decay and the small temperature dependence of the lifetimes. Under these conditions, our simulations indicate that the exciton decay is effectively trap-limited.

CONCLUSIONS

The simulations of the excitation energy migration and trapping in PS I particle with non-homogeneously broadened pigment pools have indicated that the experimental data can be obtained only if LWA pigments are collected to a cluster (RA) located close to the RC but not in direct contact. This is different from the findings of Jia et al. (1992) and Werst et al. (1992), who placed the red pigments next to the RC. It should be pointed out, however, that in their simulations they did not use the very low energy pigments that we found necessary to include for the description of the PS I core particles from *Synechococcus* sp. Our data also support the conclusion by Werst et al. (1992) that a funnel model does not explain the experimental data.

The calculated spectra are very sensitive to the RA–RC environment, while the main pigment pool arrangement is not critical for obtaining the longest two lifetimes and their DAS. However, if type 5 pigments are spread in the lattice as, for example, in pattern M, this main pigment pool arrangement gives rise to an ~0.8-ps lifetime with positive/negative going DAS that are in line with transient absorption evidence. It is worth noting here the importance of the steady-state fluorescence spectrum as a sensitive parameter for finding the proper lattice arrangement. We have found several different lattice arrangements which quite reasonably described the experimental DAS. However, all except one could be rejected because of the pronounced shoulder that was predicted on the blue side of the steady-state fluorescence spectrum that is not observed experimentally.

Our simulations, which are based on a large body of experimental data from a well-defined PS I preparation, give detailed insight into the excitation equilibration and trapping processes in PS I core particles. Most of our conclusions are in line with recent experimental findings of several other groups with regard to the very rapid excitation equilibration of a few picoseconds in the main pigment pool (Jia et al., 1992; Owens et al., 1988; Causgrove et al., 1989; Klug et al., 1989; Evans et al., 1990; Lin et al., 1992; Holzwarth et al., 1990, 1993). The simulations with varying numbers of LWA pigments clearly indicate the importance of the energetic distribution of pigments as compared with the total antenna size for the overall trapping time. This point has not been examined in previous work that studied the relationship between the trapping time and the antenna size in PS I particles (Owens et al., 1987, 1988). Despite some success in describing experimental data, a number of problems and peculiarities in these simulations remain to be studied. Among those problems, in particular, the very high charge separation rate constant k_{RC} that was necessary in our simulations deserves particular attention. Furthermore, the proper dimensionality of the energy transfer topography remains to be clarified.

We acknowledge Mr. D. Sonnenschein for support with programming and Prof. K. Schaffner for interest and support of this work.

G.T. gratefully acknowledges a research fellowship from the Deutsche Forschungsgemeinschaft (Cooperation Program with Eastern Europe), which supported his stay at the Max-Planck-Institut, Mülheim.

REFERENCES

Bassi, R., G. Hoyer-Hansen, R. Barbato, G. M. Giacometti, and D. J. Simpson. 1987. Chlorophyll-proteins of the photosystem II antenna system. *J.*

Biol. Chem. 262:13333–13341.

Beauregard, M., I. Martin, and A. R. Holzwarth. 1991. Kinetic modelling of exciton migration in photosynthetic systems. 1. Effects of pigment heterogeneity and antenna topography on exciton kinetics and charge separation yields. *Biochim. Biophys. Acta.* 1060:271–283.

Boekema, E. J., J. P. Dekker, M. Rögner, I. Witt, H. T. Witt, and M. van Heel. 1989. Refined analysis of the trimeric structure of the isolated photosystem I complex from the thermophilic cyanobacterium *Synechococcus* sp. *Biochim. Biophys. Acta.* 974:81–87.

Boettcher, B., P. Gräber, and E. J. Boekema. 1992. The structure of photosystem I from the thermophilic cyanobacterium *Synechococcus* sp. determined by electron microscopy of two-dimensional crystals. *Biochim. Biophys. Acta.* 1100:125–136.

Brown, J. S., and S. Schoch. 1981. Spectral analysis of chlorophyll-protein complexes from higher plant chloroplasts. *Biochim. Biophys. Acta.* 636: 201–209.

Butler, W. L. 1961. A far-red absorbing form of chlorophyll, in vivo. *Arch. Biochem. Biophys.* 93:413–422.

Causgrove, T. P., S. M. Yang, and W. S. Struve. 1988. Electronic excitation transport in core antennae of enriched photosystem I particles from spinach chloroplasts. *J. Phys. Chem.* 92:6121–6124.

Causgrove, T. P., S. Yang, and W. S. Struve. 1989. Polarized pump-probe spectroscopy of photosystem I antenna excitation transport. *J. Phys. Chem.* 93:6844–6850.

Du, M., X. Xie, Y. Jia, L. Mets, and G. R. Fleming. 1993. Direct observation of ultrafast energy transfer in PSI core antenna. *Chem. Phys. Lett.* 201: 535–542.

Evans, E. H., R. Sparrow, and R. G. Brown. 1990. Picosecond absorption measurements of photosystem I from the cyanobacterium *Chlorogloea fritschii. In* Current Research in Photosynthesis. M. Baltscheffsky, editor. Kluwer Academic Publishers, Dordrecht, The Netherlands. 615–618.

Förster, T. 1949. Experimentelle und theoretische Untersuchung des zwischenmolekularen Übergangs von Elektronenanregungsenergie. *Z. Naturforsch.* 4a:321–327.

Förster, T. 1965. 1. Delocalized excitation and excitation transfer. *In* Modern Quantum Chemistry, Part II, B1. O. Sinanoglu, editor. Academic Press, New York. 93–137.

Friedrich, J., and D. Haarer. 1984. Photochemical hole burning and optical relaxation spectroscopy in polymers and glasses. *Angew. Chem. Int. Ed. Engl.* 96:96–123.

Golbeck, J. H. 1993. Structure and function of photosystem I. *Annu. Rev. Plant Mol. Biol.* 43:293–324.

Gudowska-Nowak, E., M. D. Newton, and J. Fajer. 1993. Conformational and environmental effects on bacteriochlorophyll optical spectra: correlations of calculated spectra with structural results. *J. Phys. Chem.* 94: 5795–5801.

Gulyayev, B. A., and V. L. Teten'kin. 1981. Spectral anisotropy of the chloroplasts, subchloroplast particles and pigment-protein complexes. *Biophysics.* 26:291–298.

Hanson, L. K., and J. Fajer. 1987. Effects of protein solvation on the properties of bacteriochlorophylls. Theoretical studies. *Biophys. J.* 51:379. (Abstr.)

Holzwarth, A. R., J. Wendler, and G. W. Suter. 1987. Studies on chromophore coupling in isolated phycobiliproteins. II. Picosecond energy transfer kinetics and time-resolved fluorescence spectra of C-phycocyanin from *Synechococcus* 6301 as a function of the aggregation state. *Biophys. J.* 51:1–12.

Holzwarth, A. R., W. Haehnel, R. Ratajczak, E. Bittersmann, and G. H. Schatz. 1990. Energy transfer kinetics in photosystem I particles isolated from *Synechococcus* sp. and from higher plants. *In* Current Research in Photosynthesis. M. Baltscheffsky, editor. Kluwer Academic Publishers, Dordrecht, The Netherlands. 611–614.

Holzwarth, A. R., G. Schatz, H. Brock, and E. Bittersmann. 1993. Energy transfer and charge separation kinetics in photosystem I: 1. Picosecond transient absorption and fluorescence study of cyanobacterial photosystem I particles. *Biophys. J.* 64:1813–1826.

Jean, J. M., C.-K. Chan, G. R. Fleming, and T. G. Owens. 1989. Excitation transport and trapping on spectrally disordered lattices. *Biophys. J.* 56: 1203–1215.

Jia, Y., J. M. Jean, M. M. Werst, C. Chan, and G. R. Fleming. 1992. Simulations of the temperature dependence of energy transfer in the PS I core antenna. *Biophys. J.* 63:259–273.

Kenkre, V. M., and R. S. Knox. 1974a. Generalized-master-equation theory of excitation transfer. *Physical Review B.* 9:5279–5290.

Kenkre, V. M., and R. S. Knox. 1974b. Theory of fast and slow excitation transfer rates. *Phys. Rev. Lett.* 33:803–806.

Klug, D. R., L. B. Giorgi, B. Crystall, J. Barber, and G. Porter. 1989. Energy transfer to low energy chlorophyll species prior to trapping by P700 and subsequent electron transfer. *Photosynth. Res.* 22:277–284.

Knox, R. S. 1968. On the theory of trapping of excitation in the photosynthetic unit. *J. Theor. Biol.* 21:244–259.

Knox, R. S. 1975. Excitation energy transfer and migration: theoretical considerations. *In* Bioenergetics of Photosynthesis. Govindjee, editor. Academic Press, New York. 183–221.

Krauss, N., W. Hinrichs, I. Witt, P. Fromme, W. Pritzlow, Z. Dauter, C. Betzel, K. S. Wilson, and W. Saenger. 1993. Three-dimensional structure of system I of photosynthesis at 6A resolution. *Nature (Lond.).* 361: 326–331.

Kuang, T.-Y., J. H. Argyroudi-Akoyunoglou, H. Y. Nakatani, J. Watson, and C. J. Arntzen. 1984. The origin of the long-wavelength fluorescence emission band (77 degrees K) from photosystem I. *Arch. Biochem. Biophys.* 235:618–627.

Kudzmauskas, S., L. Valkunas, and A. Y. Borisov. 1983. A theory of excitation transfer in photosynthetic units. *J. Theor. Biol.* 105:13–23.

Kühlbrandt, W., and K. H. Downing. 1989. Two-dimensional structure of plant light-harvesting complex at 3.7 A resolution by electron crystallography. *J. Mol. Biol.* 207:823–828.

Kühlbrandt, W., and D. N. Wang. 1991. Three-dimensional structure of plant light-harvesting complex determined by electron crystallography. *Nature (Lond.).* 350:130–134.

Lee, H. W. H., C. A. Walsh, and M. D. Fayer. 1985. Inhomogeneous broadening of electronic transitions of chromophores in crystals and glasses: analysis of hole burning and fluorescence line narrowing experiments. *J. Chem. Phys.* 82:3948–3958.

Lin, S., H. Van Amerongen, and W. S. Struve. 1992. Ultrafast pump-probe spectroscopy of the P700-and Fx-containing photosystem I core protein from *Synechococcus* sp. PCC 6301 (*Anacystis nidulans*). *Biochim. Biophys. Acta.* 1140:6–14.

Matthews, B. W., and R. E. Fenna. 1980. Structure of a green bacteriochlorophyll protein. *Accounts in Chemical Research* 13:309–317.

Montroll, E. W. 1969. Random walks on lattices. III. Calculation of first passage times with application to exciton trapping on photosynthetic units. *J. Math. Phys.* 10:753–765.

Owens, T. G., S. P. Webb, L. Mets, R. S. Alberte, and G. R. Fleming. 1987. Antenna size dependence of fluorescence decay in the core antenna of photosystem I: estimates of charge separation and energy transfer rates. *Proc. Natl. Acad. Sci. USA.* 84:1532–1536.

Owens, T. G., S. P. Webb, R. S. Alberte, L. Mets, and G. R. Fleming. 1988. Antenna structure and excitation dynamics in photosystem I. I. Studies of detergent-isolated photosystem I preparations using time-resolved fluorescence analysis. *Biophys. J.* 53:733–745.

Parson, W. W. 1991. Reaction centers. *In* Chlorophylls. H. Scheer, editor. CRC Press, Boca Raton, FL. 1153–1180.

Pearlstein, R. M. 1982a. Exciton migration and trapping in photosynthesis. *Photochem. Photobiol.* 35:835–844.

Pearlstein, R. M. 1982b. Chlorophyll singlet excitons. *In* Photosynthesis. Govindjee, editor. Academic Press, New York. 293–331.

Pearlstein, R. M. 1984. Photosynthetic exciton migration and trapping. *In* Advances in Photosynthesis Research, Vol. I.1. C. Sybesma, editor. Nijhoff, The Hague. 13–20.

Roelofs, T. A., M. Gilbert, V. A. Shuvalov, and A. R. Holzwarth. 1991. Picosecond fluorescence kinetics of the D1-D2-cyt-b559 photosystem II reaction center complex. Energy transfer and primary charge separation processes. *Biochim. Biophys. Acta.* 1060:237–244.

Roelofs, T. A., C.-H. Lee, and A. R. Holzwarth. 1992. Global target analysis of picosecond chlorophyll fluorescence kinetics from pea chloroplasts. A new approach to the characterization of the primary processes in photosystem II alpha- and beta-units. *Biophys. J.* 61:1147–1163.

Rögner, M., U. Mühlenhoff, E. J. Boekema, and H. T. Witt. 1990. Mono-, di- and trimeric PS I reaction center complexes isolated from the thermophilic cyanobacterium *Synechococcus* sp. Size, shape and activity. *Biochim. Biophys. Acta.* 1015:415–424.

Schatz, G. H., H. Brock, and A. R. Holzwarth. 1987. Picosecond kinetics of fluorescence and absorbance changes in photosystem II particles excited at low photon density. *Proc. Natl. Acad. Sci. USA*. 84:8414–8418.

Schatz, G. H., H. Brock, and A. R. Holzwarth. 1988. A kinetic and energetic model for the primary processes in photosystem II. *Biophys. J.* 54:397–405.

Shiozawa, J. A., R. S. Alberte, and J. P. Thornber. 1974. The P700-chlorophyll a-protein isolation and some characteristics of the complex in higher plants. *Arch. Biochem. Biophys.* 165:388–397.

Shipman, L. L., T. M. Cotton, J. R. Norris, and J. J. Katz. 1976. An analysis of the visible absorption spectrum of chlorophyll a monomer, dimer, and oligomers in solution. *J. Am. Chem. Soc.* 98:8222–8230.

Strasser, R. J., and W. L. Butler. 1977. Fluorescence emission spectra of photosystem I photosystem II and the light-harvesting chlorophyll a/b complex of higher plants. *Biochim. Biophys. Acta*. 462:307–313.

Strickler, S. J., and R. A. Berg. 1962. Relationship between absorption intensity and fluorescence lifetime of molecules. *J. Chem. Phys.* 37:814–822.

Suter, G. W., and A. R. Holzwarth. 1987. A kinetic model for the energy transfer in phycobilisomes. *Biophys. J.* 52:673–683.

Thornber, J. P., J. P. Markwell, and S. Reinman. 1979. Plant chlorophyll-protein complexes: recent advances. *Photochem. Photobiol.* 29:1205–1216.

Trissl, H.-W., B. Hecks, and K. Wulf. 1993. Invariable trapping times in photosystem I upon excitation of minor long-wavelength absorbing pigments. *Photochem. Photobiol.* 57:108–112.

Turconi, S., G. Schweitzer, and A. R. Holzwarth. 1993a. Temperature dependence of picosecond fluorescence kinetics of a cyanobacterial photosystem I particle. *Photochem. Photobiol.* 57:113–119.

Turconi, S., N. Weber, G. Schweitzer, H. Strotmann, and A. R. Holzwarth. 1994. Energy transfer and charge separation kinetics in photosystem 1. 2. Picosecond fluorescence study of various PSI particles and light-harvesting complex isolated from higher plants. *Biochim. Biophys. Acta.*, in press.

van Grondelle, R., and J. Amesz. 1986. Excitation energy transfer in photosynthetic systems. *In* Light Emission by Plants and Bacteria. Govindjee, J. Amesz, and D. C. Fork, editors. Academic Press, New York. 191–224.

van Grondelle, R., H. Bergström, V. Sundström, R. J. van Dorssen, M. Vos, and C. N. Hunter. 1988. Excitation energy transfer in the light-harvesting antenna of photosynthetic purple bacteria: the role of the long-wavelength absorbing pigment B896. *In* Photosynthetic Light-Harvesting Systems. H. Scheer and S. Schneider, editors. de Gruyter, Berlin. 519–530.

Wasielewski, M. R., D. G. Johnson, M. Seibert, and Govindjee. 1989. Determination of the primary charge separation rate in isolated photosystem II reaction centers with 500-fs time resolution. *Proc. Natl. Acad. Sci. USA*. 86:524–528.

Werst, M., Y. W. Jia, L. Mets, and G. R. Fleming. 1992. Energy transfer and trapping in the photosystem I core antenna. A temperature study. *Biophys. J.* 61:868–878.

Witt, I., H. T. Witt, D. Di Fiore, M. Rögner, W. Hinrichs, W. Saenger, J. Granzin, C. Betzel, and Z. Dauter. 1988. X-ray characterization of single crystals of the reaction center I of water splitting photosynthesis. *Ber. Bunsen-Ges. Phys. Chem.* 92:1503–1506.